

IFSCC 2025 full paper (IFSCC2025-607)

Soothing and repairing effects and mechanisms of *Tricholoma matsutake* extracts on sensitive skin

Huixian Xu ¹, Lu Hu ¹, Lanyue Zhang ², Chujie Huang ^{1,*}

¹ SHE LOG (Guangzhou) Biotechnology Co., Ltd, Guangzhou 510080, China;

² School of Biomedical and Pharmaceutical Sciences, Guangdong University of Technology, Guangzhou 510006, China.

1. Introduction

Differences in structural and functional skin characteristics have been linked with ethnical background.^[1] Asian skin is characterized by low maturity and a fragile skin barrier prone to sensitivity.^[2,3] The barrier function regulates trans epidermal water loss (TEWL) and prevents the infiltration of poisonous, sensitizing, or irritating substances into the living layers of the skin. Consequently, the skin's responsiveness to external stimuli is significantly influenced by the integrity of the skin barrier.^[4,5] Skin damage represents a ubiquitous occurrence in daily life, stemming from a myriad of external and internal triggers, which impact multiple layers of skin, ranging from the epidermis to the dermis and subcutaneous layers.^[4,6] Post skin injury, the body liberates inflammatory mediators such as histamine, prostaglandins, and cytokines to beckon immune cells to the site of damage, expunging pathogens and compromised tissue.^[7] Despite its pivotal role in healing, an excessive or persistent inflammatory response can precipitate delayed healing or scar tissue formation.^[8] Prompt action and suitable care are crucial for promoting skin regeneration and preventing infections, making soothing and reparative effects crucial in cosmetics.

Sustaining the equilibrium of reactive oxygen species (ROS) and antioxidant systems like superoxide dismutase (SOD),^[9] fortifying the skin barrier function, fostering collagen synthesis, mitigating oxidative stressors such as malondialdehyde (MDA),^[10] preserving adequate hydration levels, and catalyzing hyaluronic acid (HA) synthesis stand as critical facets in the alleviation of skin inflammation and the process of skin repair.^[11,12] Furthermore, the augmentation of hyaluronic acid (HA) synthesis can serve to enhance skin moisturization and reparative capabilities. Cosmeceuticals designed for soothing and reparative purposes are cosmetic formulations tailored to address specific skin concerns. Plateau rare plants, growing in extremely high-altitude environments with intense UVB radiation, severe cold, and hypoxia, evolve to enrich "adaptogenic" substances, gaining strong resistance and adaptability to withstand external stress damage.^[13] *Tricholoma matsutake* is a rare and valuable fungus thriving in pristine, high-altitude forests. It contains abundant nutritional actives and medical properties^[14,15], making it increasingly popular in cosmetics for soothing and repairing purposes.^[14,16] Recent cosmetic research has smoothly merged *T. matsutake* and its derivatives. Pioneering research by Hu et al. sheds light on the potent synergy of *T. matsutake* extract combined with bakuchiol and ergothioneine, effectively combating

UVB-induced skin aging.^[17] However, the underlying mechanism behind *T. matsutake*'s soothing and repairing efficacy remains unknown.

This study aimed to examine the mechanism of *T. matsutake* extract (TME) in skin soothing and repairing by assessing safety by hemolytic reaction and investigating the inhibitory effects on ROS, NO, and other inflammatory factors in RAW264.7 macrophages. Simultaneously, alterations in the HaCaT cellular structure were examined using laser confocal microscopy, while ELISA was employed to measure the impacts on hyaluronic acid, collagen, and ceramide expression. This study presents compelling evidence of the considerable potential of *T. matsutake* as a natural resource in the food, cosmetics, and pharmaceutical industries, thereby fostering the sustainable growth of rare species.

2. Materials and Methods

2.1. Reagents and Materials

Aseptic sheep blood devoid of fibers. Test kits purchased from Edsen Biotechnology Co., Ltd. (Jiangsu, China). Other chemical reagents are of analytical grade and provided by Aladdin Reagent Co., Ltd. (Shanghai, China).

2.2. Cell Culture

Human immortalized keratinocytes (HaCaT) and RAW264.7 cells were cultured in high-glucose DMEM medium containing 10% fetal bovine serum at 37°C in a cell culture incubator with 5% CO₂. Cells in stable growth and logarithmic growth phases were selected for subsequent experiments.

2.3. TME Hemolytic Test

Transfer 1 mL of sterile defibrinated sheep blood into a 15 mL centrifuge tube, add 8 mL of 37°C PBS, mix thoroughly, and centrifuge at 3800 rpm for 15 minutes to remove proteins from the supernatant, repeating this process three times. Add 10 mL of 37°C PBS and set up different treatment groups: control group (PBS), total hemolysis group (deionized water), *T. matsutake* extract group (30, 15, 7.5, and 3.875 mg/mL) mixed with red blood cell suspension in equal volumes and cultured at 37°C for 1 hour. Terminate the reaction by centrifugation at 1000 rpm for 5 minutes. Take the supernatant and measure the absorbance at 560 nm to calculate the hemolysis rate.

2.4. RAW264.7 Cells ROS release assay

RAW264.7 cells were retrieved from liquid nitrogen, resuscitated, passaged, and expanded for two to three generations. When the cell viability was optimal, 100 µL of cell suspension was added to each well of a 96-well plate. 24 hours later, the cells adhered and the old culture medium was removed. Then 1 mL of a complete medium with varied TME concentrations was added. The experimental groups included control (no LPS), LPS (LPS), DXM (LPS + SDS), TME-H (LPS + 500 µg/mL TME), TME-M (LPS + 250 µg/mL TME), and TME-L (LPS + 125 µg/mL TME). After 24 hours, the cells were stained with 10 µM 2',7'-dichlorofluorescin diacetate (DCFH-DA) and incubated at 37°C, 5% CO₂ for 60 minutes. Cells were observed under inverted fluorescence microscopes with a 488 nm excitation wavelength.

2.5. RAW264.7 Cells NO Release Assay

The RAW264.7 cells received the same treatment for 24 hours. After removing the old culture medium, 1 mL of complete media with varied TME concentrations was added. The experimental groups included control (no LPS), LPS (LPS), DXM (LPS + dexamethasone), TME-H (LPS + 500 µg/mL TME), TME-M (LPS + 250 µg/mL TME), and TME-L (LPS + 125 µg/mL TME). Following treatment, the Beyotime NO detection kit instructions were followed. Standard compounds were diluted in serum-free DMEM to concentrations of 0, 1, 2, 5, and 10 µM. Griess reagents I and II were added per kit directions. The standard curve from the standard product concentrations was used to compute NO concentrations using optical density (OD) values at 540 nm.

2.6. RAW264.7 Cells ELISA Assay

RAW264.7 cells were subjected to operations according to the instructions of the Biotian ELISA assay kit. HRP-conjugated IL-6, TNF-α, and IL-1 antibodies were added to the cell supernatant, followed by a 1-hour incubation at 37°C. The wells were washed three times with PBS, and 100 µL of chromogenic reagent was added to each well for a 15-minute color development. Following color development, 100 µL of stop solution was added to each well, and the OD value was immediately measured at 450 nm.

2.7. HaCaT Cells Migration Experiment

HaCaT Cells were cultivated in a 37°C, 5% CO₂ incubator. After 24 hours, the wells were filled with media containing various medication doses, including control, UV (40 mJ/cm²), VC (125 µg/mL), TME-H (500 µg/mL), TME-M (250 µg/mL), and TME-L (125 µg/mL). The culture plate was placed in a 37°C, 5% CO₂ incubator to grow cells. A microscope was used to photograph the cell scratch wounds at 0 and 24 hours after replacing the media with PBS. Four fields per well were selected. Cell migration rate was estimated using the formula (initial scratch width - post-cultivation scratch width) / initial scratch width × 100%.

2.8. HaCaT Cells Cytoskeleton Experiment

HaCaT cells were fixed with cell fixation solution for 10 minutes, permeabilized with 0.5% Triton-X100 for 10 minutes, and washed three times with PBS. TRITC-labeled phalloidin was then added to the dish and incubated at room temperature in the dark for 30 minutes. 10 µg/mL DAPI solution was applied to the dish for dark staining for 10 minutes. Antifade mounting medium was added to the dish, and images were captured under a confocal microscope.

2.9. HaCaT Cells ELISA Assay

Add basic medium with TME concentrations for control, UV, and VC groups to the wells. Drug concentration gradients of 500, 250, and 125 µg/mL are used, with three replicates per group. The HaCaT cells were cultured in the 37°C, 5% CO₂ incubator. After 24 hours, place the 24-well plate on ice, add 100 µL RIPA lysis buffer to each well, and incubate for 30 minutes. Then, centrifuge the whole cellular protein solution at 4°C/3000 rpm for 10 minutes. Measure supernatant COL, HA, CER, SOD, and MDA with ELISA kits.

2.10. Statistical Analysis

Data were presented as the mean ± standard error. All statistical analyses were performed using GraphPad Prism 8.0.2 statistical software. One-factor analysis of variance was used to compare the means of multiple groups. A two-sided Student T-test was used for

pairwise comparison between small groups. p-Value < 0.05 was considered statistically significant (*p < 0.05). p-values < 0.01 were considered a significant difference.

3. Results

3.1. TME Hemolytic Test

Skin allergy arises from an aberrant immune response to substances (allergens) that ordinarily do not provoke adverse effects. Hemolysis denotes the rupture of red blood cells, resulting in the release of hemoglobin and other intracellular constituents. Allergic responses can occasionally induce hemolysis. In allergic hemolytic anemia, allergens can stimulate the immune system to target and destroy autologous red blood cells, resulting in their lysis and the release of hemoglobin.

According to YY/T 1532-2017, a hemolysis rate below 5% indicates non-hemolysis. As illustrated in Figure 1, when the concentrations of TME \leq 15 mg/mL, the hemolysis rate was < 5%, demonstrating excellent low blood compatibility. A low hemolysis rate indicated minimal damage to red blood cells, thereby not eliciting significant hemolytic reactions. However, at a concentration of 30 mg/mL, although the overall hemolysis rate significantly increased compared to 15 mg/mL, it was still below the specified 5% standard. Therefore, at dosages below 30 mg/mL, TME exhibited favorable low blood compatibility.

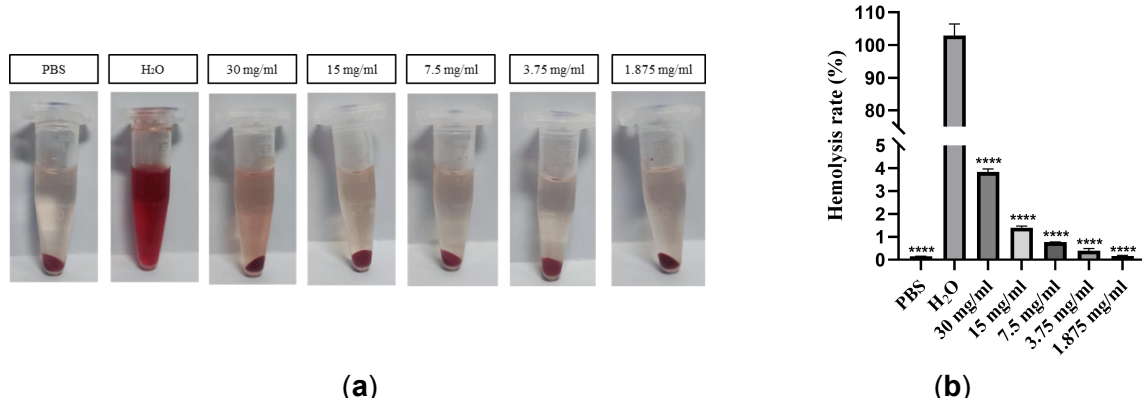


Figure 1. Hemolytic test of TME. (a) Hemolysis test images of TME; (b) Quantitative analysis of the hemolysis rate of TME.

3.2. RAW264.7 Cells assay of ROS and NO release

As shown in Figure 2a, ROS detection results showed significant differences among treatment groups. Specifically, IOD dramatically increased (1402.0 ± 190.7) in the LPS treatment group, demonstrating a strongly inducible effect on ROS generation. Control group IOD (129.1 ± 82.1) showed the lowest ROS activity without a stimulant. While ROS generation was effectively reversed in the DXM group ($p < 0.01$), the TME group showed a superior effect. In the TME treatment groups, all three dose groups showed inhibition of ROS generation. Moreover, the IOD value of the high-dose TME group was similar to that of the control group, indicating that TME effectively suppressed the production of ROS and regulated the ROS level in a dose-dependent manner.

Nitric oxide (NO) regulates skin cell proliferation, differentiation, death, inflammation, and immunological responses. UV light activates skin cell nitric oxide synthase (NOS), thereby increasing NO production. The LPS group had considerably higher NO levels than the control group ($p < 0.05$), validating the efficacy of this modeling approach. Figure 2b shows that all

three TME dosages significantly reduced NO levels compared to the LPS group ($p < 0.05$). Notably, higher concentrations of TME exerted a robust inhibitory effect on NO activity ($p < 0.01$). These data indicated TME protected against LPS induced inflammation at certain concentrations.

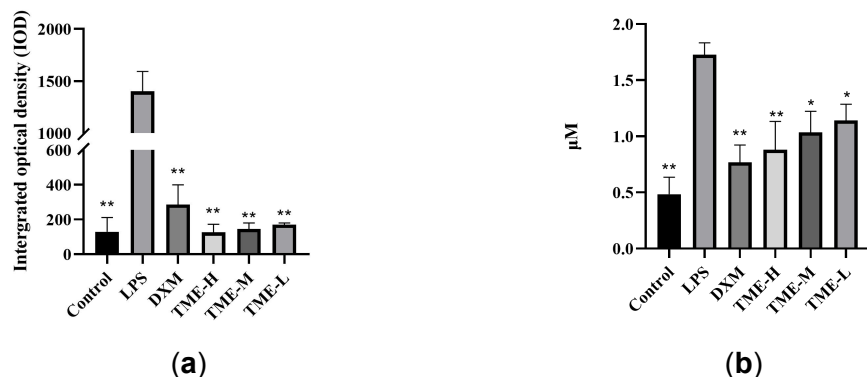


Figure 2. Effect of ROS and NO content in RAW264.7 cells. Quantitative analysis of the effect of ROS (a) and NO (b) content in RAW264.7 cells (* $p < 0.05$ and ** $p < 0.01$).

3.3. RAW264.7 Cells ELISA Assay

When the skin is damaged by external stimuli, inflammatory factors such as IL-1, IL-6, and TNF- α significantly increase. These factors activate immune cells in the skin through signal transduction pathways, triggering or exacerbating inflammatory reactions in the skin. Compared to the control group, LPS stimulation led to a notable elevation in levels of inflammatory cytokines, particularly TNF- α and IL-1 ($p < 0.01$). The results indicated that the inhibitory effect of TME on the secretion of inflammatory factors is dose-dependent, with a more pronounced inhibition observed of TNF- α and IL-1 ($p < 0.01$). Notably, at higher concentrations, TME demonstrates a more pronounced inhibitory effect on TNF- α , IL-1, and IL-6 (Figure 3).

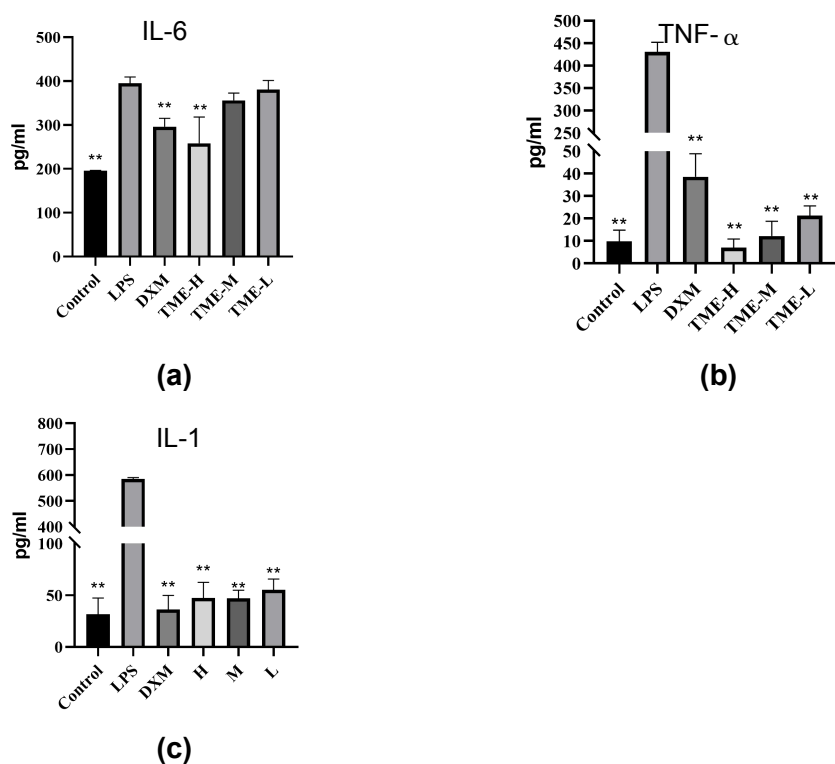


Figure 3. Effect of *T. matsutake* on IL-6, TNF- α , and IL-1 production induced by LPS. The levels of IL-6 (a), TNF- α (b), and IL-1 (c) in RAW264.7 cells were examined by the ELISA assay. (* $p < 0.05$ and ** $p < 0.01$).

3.4. HaCaT Cells Migration Experiment

The scratch assay was the most commonly used method to measure cell migration and cell repair efficacy. An artificial blank area termed a "scratch/wound" was created on a confluent monolayer of cells, and cells at the edges gradually entered the blank area, promoting "healing" of the scratch/wound. Due to its similarity to wound healing processes, this experiment has been widely employed for in vitro assessment of the repairing effects of drugs on wounds. As shown in Fig. 4, the results indicated that 24 hours after TME treatment, within the range of 125 μ g/mL to 500 μ g/mL, the cell migration rate increased with escalating TME concentrations, significantly surpassing the UV group. Moreover, after 24 hours administration of TME-H, the cells migration rate was similar to that of the VC group. The scratch migration assay results suggested that TME possessed the potential for skin injury repair.

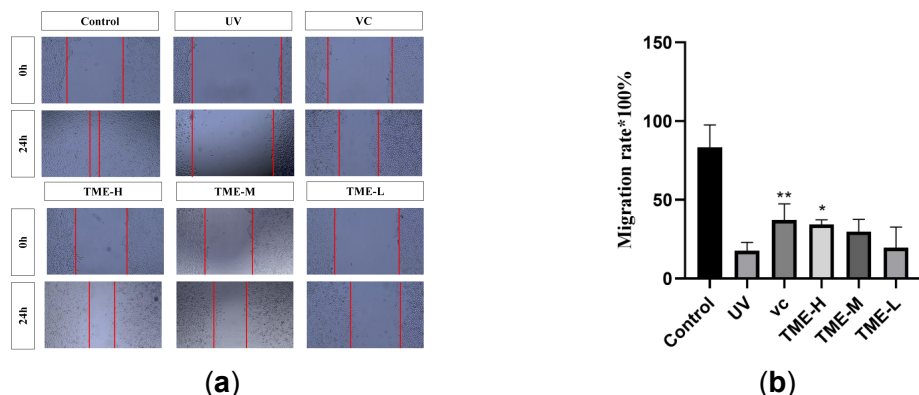


Figure 4. The effect of TME on HaCaT cell migration for 24h. (a) The images of HaCaT cell migration in each group. (b) Quantitative analysis of HaCaT cell migration rate. (* $p < 0.05$ and ** $p < 0.01$).

3.5. HaCaT Cells Cytoskeleton Experiment

The cell cytoskeleton is a network structure primarily composed of protein fibers within the cell, consisting of three main types of protein filaments: microtubules, actin filaments, and intermediate filaments. It plays a crucial role in maintaining cell shape and internal organization, influencing various cellular functions such as movement, material transport, energy conversion, signal transduction, and differentiation. As shown in Figure 5, the cytoskeleton of the control group cells appears as regular filaments, while the UV model group displays a disarrayed cytoskeleton in damaged cells. Following treatment with varying concentrations of TME, the cytoskeleton returns to a normal filamentous state, with the TME-H group demonstrating the most effective repair outcome. These findings suggest that TME can repair cell damage caused by inflammatory responses.

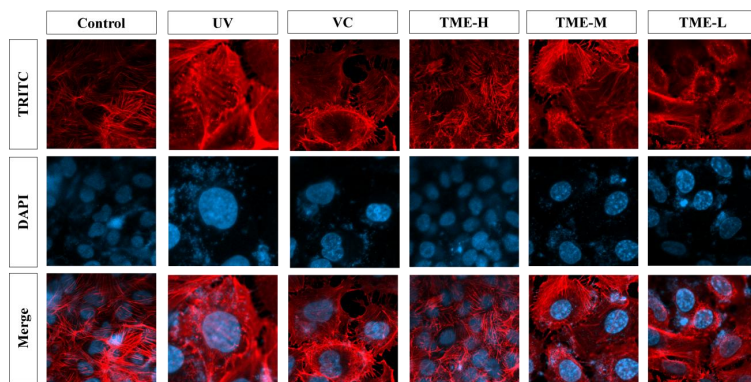


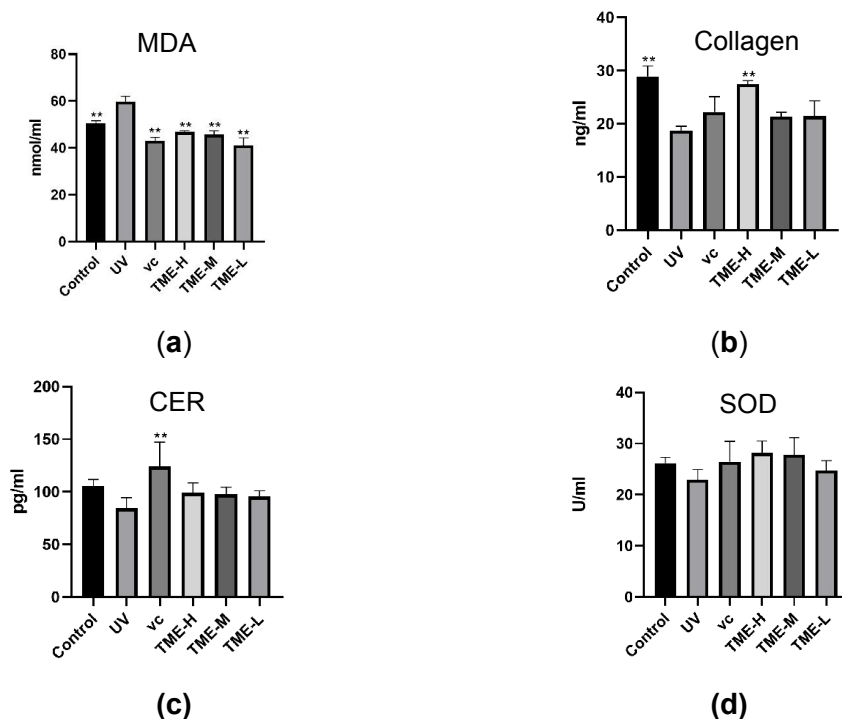
Figure 5. Effect of TME on the cytoskeleton of HaCaT

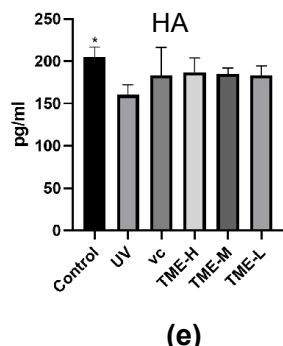
3.6. HaCaT Cells ELISA Assay

In Figure 6a, following a 24-hour cell culture with different concentrations of TME, the expression of MDA in the TME group decreased compared to the UV group, indicating a reduction in MDA levels. Skin wound healing and anti-aging also depend on collagen. Figure 6b shows that after a 24-hour cell culture with varied TME doses, collagen expression in the TME-H group increased significantly compared to the UV group ($p < 0.05$).

Ceramide maintains skin barrier function, modulates inflammatory responses, facilitates cell signaling, and provides antioxidant protection, accelerating skin tissue repair and recovery. As shown in Figures 6c and 6d, cell cultures treated with different TME doses for 24 hours showed elevation both of CER and SOD expression.

Hyaluronic acid is a common glycosaminoglycan formed by glucuronic acid and N-acetylglucosamine. As illustrated in Figure 6e, after culturing cells with varying concentrations of TME for 24 hours, the expression of hyaluronic acid in the TME group also exhibited an upward trend.





(e)

Figure 6. Effects of TME on the expressions of MDA (a), Collagen (b), CER (c), SOD (d), and HA (e) in HaCaT cells (compared with Blank group, * $p < 0.05$, ** $p < 0.01$)

4. Discussion

Smoothing and repairing skin wounds requires sophisticated tissue and cell lineage cooperation. Cell migration, proliferation, matrix deposition, remodeling, and the exact coordination of inflammation and angiogenesis are needed for the cascade. Skin macrophages form the innate immune barrier. In normal conditions, macrophage phagocytosis and antigen presentation maintain the skin's immunological barrier. HaCaT cells, produced from immortalized human keratinocytes from normal skin, develop similarly to normal keratinocytes and are independent of tumors. TME skin healing efficacy was investigated on the above cell line.

Hemolysis assay results indicate that TME has good low biocompatibility at 15 mg/mL, preventing component allergy-induced hemolytic responses during TME repair. ROS release tests show that all three dosages of TME reduce ROS formation, with the highest dose being the most potent, demonstrating that TME modulates ROS levels dose-dependently. All three dosages of TME significantly lowered NO levels ($p < 0.05$) in the NO release experiment, indicating a concentration-dependent protective effect against lipopolysaccharide-induced inflammation. Inflammatory factors such as IL-1, IL-6, and TNF- α increase after skin injury, stimulating immune cells via signal transduction pathways and worsening skin inflammation.

In the enzyme-linked immunosorbent test, post-LPS treatment increased inflammatory factor levels, with TME's inhibitory effect on inflammatory factor secretion being dose-dependent. After 24 hours of TME treatment at various dosages, the MTT cell proliferation assay showed no significant difference between the three groups, indicating minimal cell toxicity ($p < 0.01$). TME treatment at concentrations ranging from 125 to 500 μ g/mL improved the cell migration rate in the scratch migration experiment after 24 hours. The 500 μ g/mL TME group showed a similar cell migration rate to the VC group after 24 hours, indicating that TME can increase cell migration at specific concentrations, potentially boosting skin restoration.

TME-treated cells had more microfilaments and microtubules, thicker stress fibers, and more cilia than the blank control group in the laser confocal microscopy experiment. The cell skeleton reverted to a normal filamentous state. Cell mobility, chemical transport, energy conversion, information transfer, and differentiation depend on the cell skeleton. Experimental results show that TME increases cell migration by aggregating cell skeleton structures like microfilaments and microtubules toward the cell periphery, reinforcing stress fibers, and promoting the synthesis of these structures and cilia to aid skin repair after photodamage.

The ELISA experiment examined how TME affected immortalized keratinocytes' SOD, CER, COL, MDA, and HA expression. SOD neutralizes excess superoxide radicals, lowering free radical buildup and inflammation-induced free radical production to reduce skin damage. As key constituents of intercellular lipids in the stratum corneum, ceramides serve as second messenger molecules in phospholipid metabolism pathways and form the epidermal barrier, maintaining hydration, anti-aging, whitening, and treating disease. Collagen stimulates cell formation, tissue differentiation, and connective tissue proliferation, making it essential for elastic tissue and sticky substances, wound healing, and skin anti-aging. Since elevated MDA levels may affect skin cell metabolic activity and function, TME lowers MDA levels. MDA reduction boosts skin cell activity, enabling repair and regeneration. Hyaluronic acid aids wound healing by regulating protein synthesis, electrolyte diffusion, and transport. Experimental results show that TME boosts SOD, CER, COL, MDA, and HA expression in immortalized keratinocytes, dramatically boosting hyaluronic acid and collagen levels ($P<0.05$). Finally, TME may help restore skin damage.

5. Conclusion

Consequently, this study confirms that *T. matsutake* enhances the body's resistance to internal and external stress through a multi-targeted, multi-pathway mechanism as demonstrated by hemolysis assays and different indicators in cellular models. Hemolysis assay shows that TME has good low blood compatibility at 15 mg/mL, indicating a safe interaction with blood or its components during sensitive skin repair without blood coagulation, hemolysis, or other undesirable responses. In RAW264.7 cell tests, TME at all three dosages effectively reduces ROS, NO release, and inflammatory factors IL-1, IL-6, and TNF- α in macrophages. This regulating impact of TME reduces oxidative damage and inflammation, increasing cell regeneration and repair, expediting skin tissue healing, tissue formation, and skin functionality. Scratch migration and cell skeleton tests show that TME may effectively restore cell structures, increase cell migration, and promote wound repair. TME increases HA, COL, CER, and SOD secretions, reduces MDA production, reduces cellular inflammation, and speeds up repair, according to ELISA tests. Thus, *Tricholoma matsutake* extract exhibits a potent reparative effect on damaged skin barriers, exhibiting high safety levels, and holds significant potential in soothing and repairing cosmetics.

6. Reference

- [1] STEPANOVA E V, STRUBE M J. Making of a face: role of facial physiognomy, skin tone, and color presentation mode in evaluations of racial typicality[J]. The Journal of Social Psychology, 2009, 149(1): 66-81.
- [2] HARDING C R, LONG S, RICHARDSON J, et al. The cornified cell envelope: an important marker of stratum corneum maturation in healthy and dry skin[J]. International Journal of Cosmetic Science, 2003, 25(4): 157-167.
- [3] MUIZZUDDIN N, HELLEMANS L, VAN OVERLOOP L, et al. Structural and functional differences in barrier properties of African American, Caucasian and East Asian skin[J]. Journal of Dermatological Science, 2010, 59(2): 123-128.
- [4] MURPHREE R W. Impairments in Skin Integrity[J]. The Nursing Clinics of North America, 2017, 52(3): 405-417.
- [5] RAWLINGS A V. Ethnic skin types: are there differences in skin structure and function?[J]. International Journal of Cosmetic Science, 2006, 28(2): 79-93.

- [6] BATTIE C, JITSUKAWA S, BERNERD F, et al. New insights in photoaging, UVA induced damage and skin types[J]. Experimental Dermatology, 2014, 23 Suppl 1: 7-12.
- [7] BÄSLER K, BRANDNER J M. Tight junctions in skin inflammation[J]. Pflugers Archiv: European Journal of Physiology, 2017, 469(1): 3-14.
- [8] PASPARAKIS M, HAASE I, NESTLE F O. Mechanisms regulating skin immunity and inflammation[J]. Nature Reviews. Immunology, 2014, 14(5): 289-301.
- [9] WANG Y, BRANICKY R, NOË A, et al. Superoxide dismutases: Dual roles in controlling ROS damage and regulating ROS signaling[J]. The Journal of Cell Biology, 2018, 217(6): 1915-1928.
- [10] GAWEŁ S, WARDAS M, NIEDWOROK E, et al. [Malondialdehyde (MDA) as a lipid peroxidation marker][J]. Wiadomosci Lekarskie (Warsaw, Poland: 1960), 2004, 57(9-10): 453-455.
- [11] LITWINIUK M, KREJNER A, SPEYRER M S, et al. Hyaluronic Acid in Inflammation and Tissue Regeneration[J]. Wounds: A Compendium of Clinical Research and Practice, 2016, 28(3): 78-88.
- [12] CHANG W, CHEN L, CHEN K. The bioengineering application of hyaluronic acid in tissue regeneration and repair[J]. International Journal of Biological Macromolecules, 2024, 270(Pt 2): 132454.
- [13] PANOSIAN A G, EFFERTH T, SHIKOV A N, et al. Evolution of the adaptogenic concept from traditional use to medical systems: Pharmacology of stress- and aging-related diseases[J]. Medicinal Research Reviews, 2021, 41(1): 630-703.
- [14] HU L, HUANG Z, WENG J, et al.. Effect and Mechanism of *Tricholoma matsutake* Extract on UVA and UVB Radiation-Induced Skin Aging[J]. Journal of Microbiology and Biotechnology, 2025, 35: e2411085.
- [15] LI M, DONG L, DU H, et al. Potential mechanisms underlying the protective effects of *Tricholoma matsutake* singer peptides against LPS-induced inflammation in RAW264.7 macrophages[J]. Food Chemistry, 2021, 353: 129452.
- [16] ZHU W, CHEN Y, QU K, et al. Effects of *Tricholoma matsutake* (Agaricomycetes) Extracts on Promoting Proliferation of HaCaT Cells and Accelerating Mice Wound Healing[J]. International Journal of Medicinal Mushrooms, 2021, 23(9): 45-53.
- [17] HU L, WENG J, WANG Z, et al. Effect and mechanism of *Tricholoma matsutake* extract combined with bakuchiol and ergothioneine on UVB-induced skin aging[J]. Journal of Cosmetic Dermatology, 2024: jocd.16457.